Available online at www.sciencedirect.com
SCIENCE DIRECT®
International Journal of Heat and Mass Transfer 48 (2005) 2806–2813
International Journal of HEAT and MASS TRANSFER
www.elsevier.com/locate/ijhmt

Technical Note

# Influence of channel height on heat transfer augmentation in rectangular channels with two opposite rib-roughened walls

Shyy Woei Chang [a,*], Tong-Miin Liou [b], Wei-Chen Juan [b]

[a] Department of Marine Engineering, National Kaohsiung Marine University, No. 142, Hai-Chuan Road, Nan-Tzu District, 811 Kaohsiung, Taiwan, ROC
[b] Department of Power Mechanical Engineering, National Tsing Hua University, 300 Hsinchu, Taiwan, ROC

Received 25 July 2003; received in revised form 23 September 2004
Available online 21 March 2005

## 1. Introduction

Among the various engineering applications involving heat transfer augmentation in cooling passages, the repeated surface ribs are often treated as turbulence promoters to enhance heat transfer. In the past, numerous experimental works have probed into the heat transfer characteristics of rib-roughened channels, which studied the effects of rib configuration and channel cross-sectional shape on the effectiveness of surface ribs for heat transfer augmentation [1–5]. The ranges of rib geometry examined are typical of rib angles: 90°, ±60°, ±45°, rib configurations: continuous, broken and V shaped ribs with inline, staggered and criss-cross arrangements, rib height to hydraulic diameter ratio: 0.0625–0.15, rib pitch to height ratio: 8–30 and channel width-to-height ratio: 0.25–4. The results revealed from these studies have demonstrated that the effectiveness of surface ribs on heat transfer augmentation varies with the geometrical features of surface-rib and coolant-channel [1–5] and with the external forces generated in bends or by rotation. The general rib-effects on heat transfer in the ducted flow are the improved heat transfer with considerable modifications in spatial heat transfer distribution from the smooth-walled scenario. Heat transfers over the rib-roughened surfaces could be enhanced by a factor of 2–4 times of Dittus–Boelter value [6]. With the attempt to employ the rib-roughened channel for cooling of electronic chipsets in a spatially confined device such as the note-book PC and PDA, the applicable channel width-to-height ratio could exceed the published results of 0.25–4 in the open literature. The present study investigates the heat transfer characteristics in the ribbed channel with channel width-to-height ratio varying from 2.5 to 10, which has extended the previously geometric range and fallen into the applicable range for cooling application of electronic chipsets. In addition, one of the main physical drawbacks in attaining the quality heat transfer data is the three-dimensional wall conductivity effect on the temperature measurements over the rib-roughened surface. The presence of surface ribs has invalidated the one-dimensional assumption adopted by the method of transient thermochromic liquid crystal thermography (TLCT). Also it is impractical to correct the thermocouple measurement onto the rib surface from the measuring spot due to the three-dimensional wall conductivity effect. In order to avoid the three-dimensional wall conductivity effect on temperature measurements, the rib-roughened surface used by the present study is folded from a continuous 0.1 mm thick stainless steel foil, which could be electrically powered as an one-dimensional rib-roughened heating surface. As the width-to-thickness ratio of heating foil is 400 that enables the assumption of one-dimensional heat conduction from the fluid-wall interface to the external surface where the temperature fields are scanned, the corrections of wall temperature from the scanned surface to the inner surface of rib-roughened channel using the one-dimensional Fourier conduction law are in the range of 0.063–0.18 K. Nevertheless the detailed heat transfer

* Corresponding author. Tel.: +886 7 8100888x5216; fax: +886 7 5721035.
E-mail address: swchang@mail.nkmu.edu.tw (S.W. Chang).

0017-9310/$ - see front matter 
doi:10.1016/j.ijheatmasstransfer.2005.02.001

measurements over a rib-roughened surface in a channel with channel width-to-height ratios ($w/b$) greater than 4, which geometries are practical for electronics cooling and plate-type heat exchanger, are very rare. The increased three-dimensionality due to vortical flow motions with mainstream flow accelerations and decelerations as a result of the reduction in channel height, which is further complicated by the secondary flows and the modified turbulence structure induced by surface ribs, requires further study. This experimental study performs the full-field heat transfer measurements using NEC TH3101-MR infrared radiometer over an enhanced surface with periodic transverse ribs in five rectangular channels of different channel heights. Each channel performs five sets of experiments fixing the coolant mass-flow-rate and five sets of tests fixing Reynolds numbers ($Re_d$), which formulates 10 different Reynolds numbers examined in the range of 3500–25,000. Twofold of geometric variations are induced by varying the sidewall thickness, namely the channel width-to-height ratio ($w/b$) and the rib height to channel height ratio ($e/b$). The impacts of channel $w/b$ ratio, $e/b$ ratio and Reynolds number on heat transfer over the rib-roughened surface are analyzed with the attempt to generate the heat transfer correlation for the evaluation of spatially averaged Nusselt number in the repeated flow region.

## 2. Experimental details

Fig. 1 shows the constructional details of the test section. As shown, each rib-roughened surface in the rectangular test channel (1) was fitted with 10 pairs of square-sectioned transverse ribs at regular interval arranged in the staggered manner. These two ribbed heating surfaces (2) and (3) were made of the continuous 40 mm wide, 0.1 mm thick stainless steel foils. A high-current, low-voltage DC electrical power supply was directly fed through the two opposite heating foils (2) and (3) to generate the uniform flux heating condition. The heater power was adjusted to raise the central wall temperature to the level of 120 °C for each test. The various heat fluxes fed into the test section affect the entry-plane Reynolds number due to variations in fluid properties. Coolant mass flow rate was adjusted to compensate the temperature affected fluid property variations that controlled the entry-plane Reynolds number within ±1% varying range for each test. The rib-shaped heating foil (3) over which the heat transfer measurements were performed was sandwiched between two Tufnol sidewalls (4) and two Tufnol bars (5) to secure its position on the test channel. The opposite rib-shaped heating foil (2) was attached on the inner surface of a 15 mm thick Tufnol back wall (6). The complete set of test section was tightened between the plenum chamber (7) and the end Tufnol plate (8) by four draw-bolts (9). A cubic plenum of width 40 mm (7) was consolidated with the test section to simulate the abrupt entry condition. Geometric features of each rectangular test section are specified in Table 1.

The pressure and temperature of the entry air in this plenum chamber (7) were measured with a pressure transducer and a type K thermocouple (10). The inlet Reynolds number could be calculated and monitored using the measured airflow, plenum chamber pressure and flow entry temperature. At the exit plane of the rectangular coolant passage, three type K thermocouples (11) penetrated into the core of test channel at three different spanwise locations. The flow bulk temperature at the exit plane of test channel was obtained by averaging these three temperature measurements (11). It is noted that the different characteristic lengths of either channel width or hydraulic diameter provide different Reynolds numbers. Because the aim of the present study is to compare the effectiveness of a predefined ribbing geometry on heat transfer augmentation in five rectangular channels with different channel height, the characteristic length selected to define the Reynolds ($Re$) and Nusselt ($Nu$) numbers is the width of test channel that remains invariant for five different test channels. To compare with the Dittus–Boelter correlation [6] for evaluating the heat transfer augmentation, the length scale selected to define Reynolds ($Re_d$) and Nusselt ($Nu_d$) numbers becomes hydraulic diameter ($d$). The flow circuit, flow measurement and data acquisition systems along with the descriptions for conducting heat loss and heat transfer experimental procedures and the method of data reduction have been previously reported [7]. Following the policy of ASME on reporting the uncertainties in experimental measurements and results [8], the maximum uncertainty associated with the local Nusselt and Reynolds numbers were estimated to be 11.6% and 5.8%, respectively.

## 3. Results and discussion

The isolines of Nusselt number over rib-roughened surface at coolant mass flow rate of 0.00323 kg/s are compared in Fig. 2 to unravel the impacts of channel height on heat transfers over the ribbed floor. The regionally high heat transfers over five ribbed floors consistently develop at the top surface of each rib. This result agrees with the measurement of real-time holographic interferometry [2] that has been attributed to the highly unsteady eddies induced on the top-face of each rib [9]. Immediate downstream of each rib emerges the regionally minimum heat transfer valley. This minimum heat transfer region, located in the recirculation zones behind each rib, undergoes near-wall streamwisely reverse flows with the turbulence intensities to be considerably suppressed [4,9]. Further downstream of each minimum

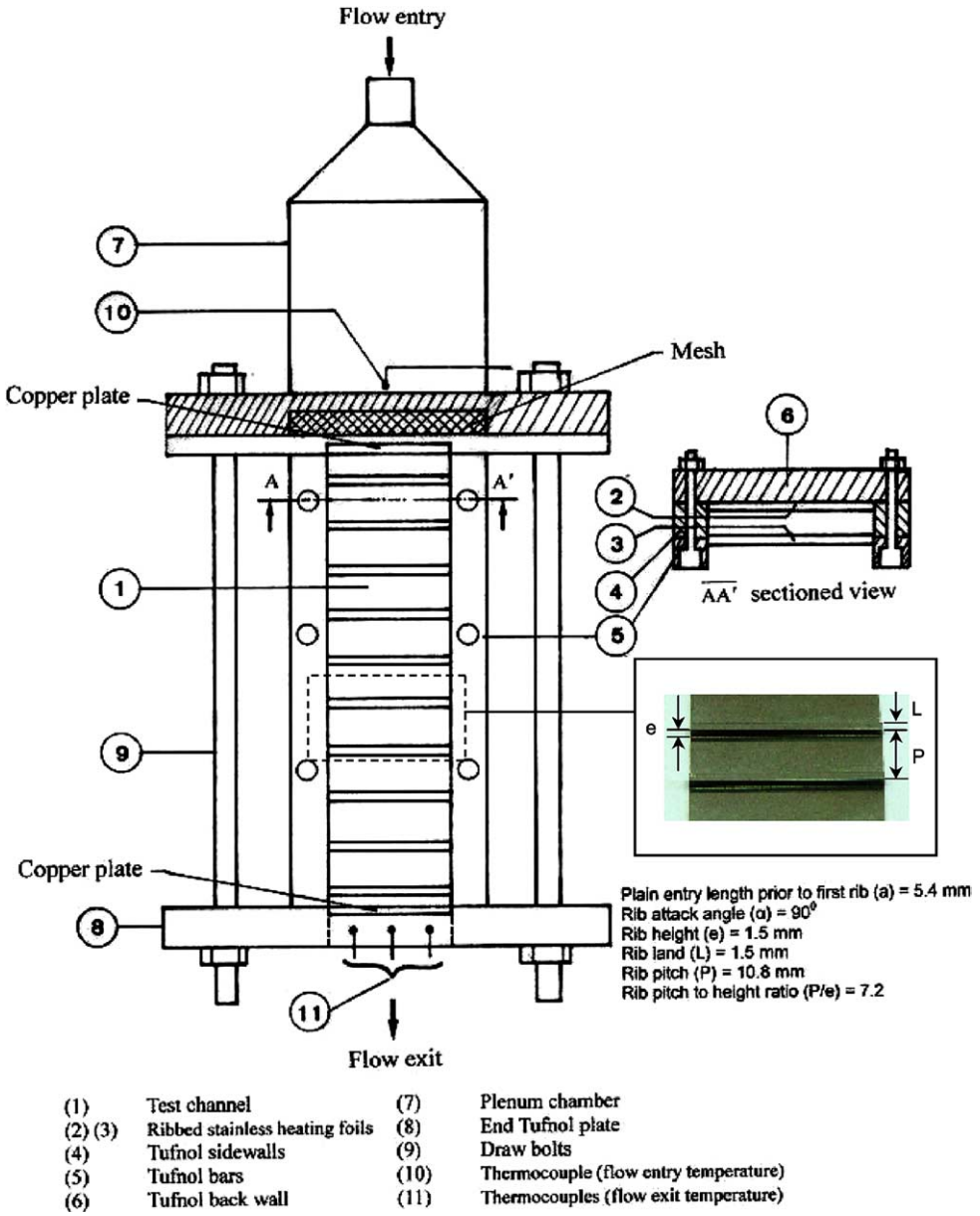


Fig. 1. Experimental apparatus.

heat-transfer band in the recirculation zone, heat transfers increase steadily in the channels of $w/b = 2.5$, 4, 5 and 6. In the channel of $w/b = 10$, there is another spanwise heat transfer peak developed at the middle of each pair of ribs. In this case, the flows triggered by the staggering ribs on two opposite walls are mutually interacted that could induce these mid-rib heat transfer peaks. As a result of the increased interactions between two opposite ribbed floors by systematically reducing the channel height, the spatially averaged Nusselt number over the entire rib-roughened surface correspondingly increases as depicted in Fig. 2. Another attribute responsible for the increased heat transfer with $w/b$ ratio is the increased Reynolds number at the fixed coolant mass flow rate due to the reduced channel cross-sectioned area.

The streamwise distributions of local Nusselt number along the centerline of each ribbed floor corresponding to the contour plots depicted in Fig. 2 are summarized in Fig. 3. At the immediate flow entrance, the locally high heat transfer is generated due to the sharp flow entrance. At this entry spot, a systematic increase in channel $w/b$ ratio from 2.5 to 10 induces the successive

Table 1
Geometrical specification of test channels

Rib configuration
Plain entry length prior to first rib ($a$) = 5.4 mm
Rib attack angle ($\alpha$) = 90° (Ribs on two opposite walls are offset by 0.5 pitch)
Rib height ($e$) = 1.5 mm
Rib land ($L$) = 1.5 mm
Rib pitch ($P$) = 10.8 mm
Rib pitch to height ratio ($P/e$) = 7.2

*Test channel configurations*

| Tested module | Channel width ($w$) (mm) | Channel height ($b$) (mm) | Channel hydraulic diameter ($d$) (mm) | Channel width to height ratio ($w/b$) | Rib height to channel height ratio ($e/b$) | Rib height to channel hydraulic diameter ratio ($e/d$) |
|---|---|---|---|---|---|---|
| A | 40 | 16 | 22.857 | 2.5 | 0.094 | 0.066 |
| B | 40 | 10 | 16 | 4 | 0.15 | 0.094 |
| C | 40 | 8 | 13.33 | 5 | 0.1875 | 0.1125 |
| D | 40 | 6.67 | 11.43 | 6 | 0.225 | 0.131 |

increase in local Nusselt number. In the plain entry length prior to the first rib, the local Nusselt numbers gradually fall in the downstream direction. Heat transfer augmentation is initiated when the streamwise bulk flow traverses the first rib by generating a streamwise heat transfer ripple within each rib pair with the peak values on the top surface of rib. In addition to the streamwise Nusselt number oscillations triggered by these surface ribs, the rib effect could considerably elevate the overall heat transfer levels further downstream in the channels with $w/b$ ratios of 4, 5, 6 and 10. But in the channel with $w/b$ ratio of 2.5, the overall streamwise heat transfers decay asymptotically from an immediate flow entrance level towards the developed value at $e/b = 0.094$. This streamwise decay in heat transfer over the plan-entry-length of developing flow region is gradually weakened when $e/b$ ratio increases up to 0.15 after which the streamwise increase of local Nusselt number over the plain entry length occurs. In this respect, a similar trend was experimentally found in three ribbed channels of different $e/d$ ratios [10]. Nevertheless, although the channels of different $w/b$ ratios in the range of 2.5–10 perform various distributing manners of local Nusselt numbers in the developing flow regions, as depicted in Fig. 3, the repeatedly periodic heat transfer variations are likely to be developed after the bulk flow traverses about five ribs. This flow region is referred to the repeated flow region, within which the regionally high heat transfer rate in each rib-pitch develops over the top surface of each rib. The locus of heat transfer crest on the top surface of each rib develops at the leading edge of rib. Heat transfers reduce streamwisely from the leading edge value on each top surface of rib. Over the back edge of each rib, the Nusselt numbers fall radically within the bandwidth of about 0.5–1 rib height to a locally minimum value in each rib pitch. Except in the channel of $w/b = 10$, a subsequent heat transfer recovery proceeds over a downstream length about 3.5–4 rib height after the local minimum spot. In the channel of $w/b = 10$, the opposite wall effect that triggers the mid-rib heat transfer ripple provides the most considerable heat transfer impacts in the developing flow region between ribs 2 and 5. In this regard, the mid-rib heat transfer value triggered by the opposite wall effect between ribs 2 and 3 is higher than the heat transfer levels occurred on the top surfaces of ribs 2 and 3. The opposite wall effect on heat transfer is gradually alleviated in the downstream direction which has led to two ripples with equivalent Nusselt number peaks over each rib-pitch in the repeated flow region for the channel of $w/b = 10$. Because these surface ribs are arranged in the staggered manner, the locus of each mid-rib heat transfer ripple locates at about 0.5 rib pitch. Justified by the twin-ripple streamwise heat transfer distributions in the repeated flow region of channel with $w/b$ ratio of 10, the energetic, dynamic and highly unsteady eddies attached over the top surface of opposite ribs [11,12] could provide considerably interactive effects on the flow structures of recirculating cell behind each rib. The flow structure in the separation zone behind each rib [11,12] is likely to be modified by the perturbing rib located at the opposite wall with the tendency of generating another middle pitch heat transfer peak. This twin-ripple streamwise heat transfer distribution in each rib pitch could attribute to the further increase of the spatially averaged Nusselt number over the repeated flow region. Among these five test channels with the $Re$ range tested, the shallow channel with $w/b$ ratio of 10 consistently provides the highest heat transfer rates.

The heat transfer augmentation is evaluated by normalizing the local Nusselt number with respect to the level obtained in a smooth circular tube of Dittus–Boelter correlation, $Nu_\infty$ [6]. As the characteristic length selected in the Dittus–Boelter correlation for defining $Re$ and $Nu$ is the hydraulic diameter of test channel, the present data of $Re$ and $Nu$ is re-scaled into $Re_d$ and $Nu_d$ using

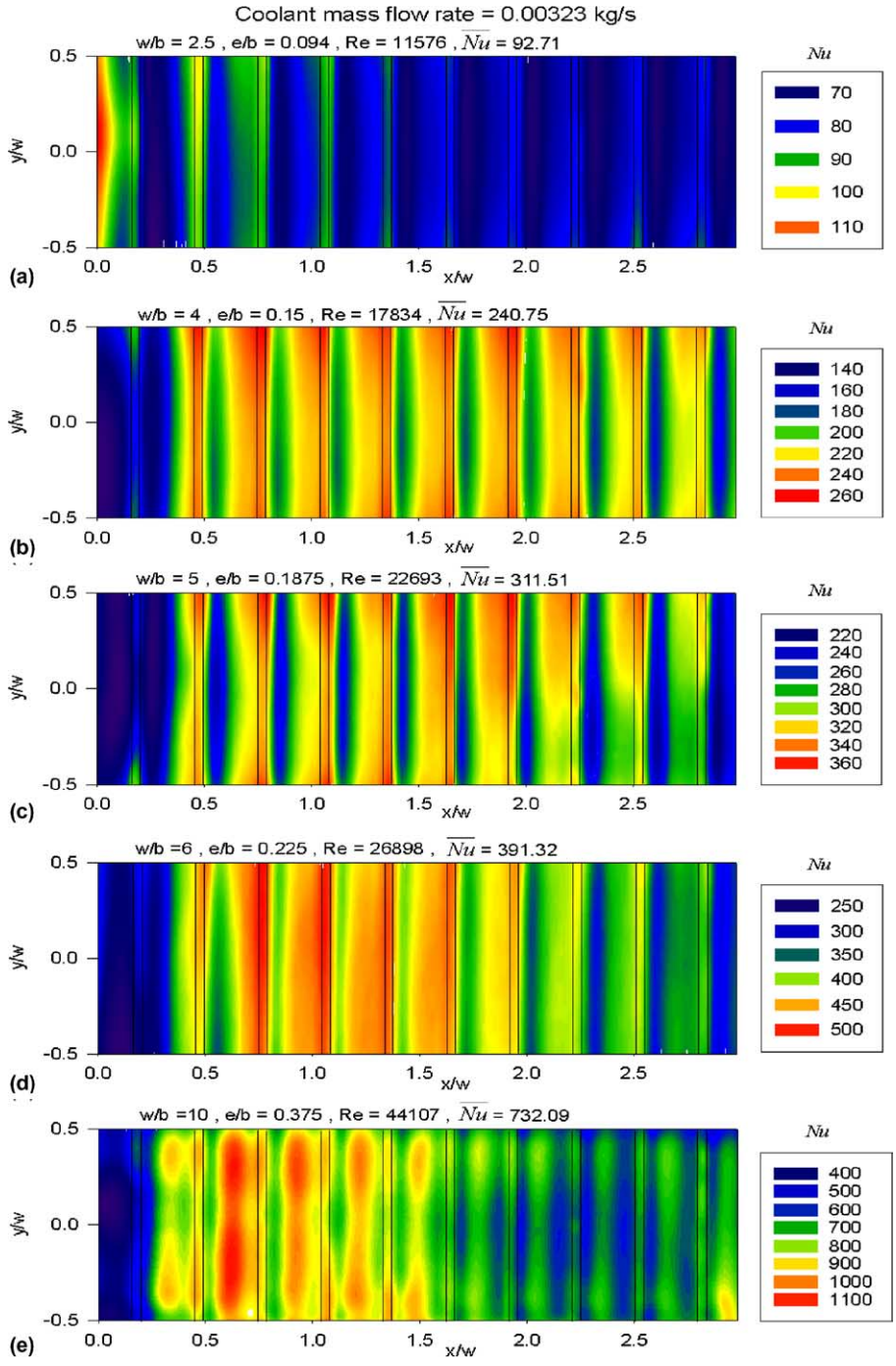


Fig. 2. Distributions of Nusselt number contours over ribbed floor in five test channels at coolant mass flow rate of 0.00323 kg/s.

the hydraulic diameter as the characteristic length. Fig. 4 shows the streamwise distributions of Nusselt number ratio, $Nu_d/Nu_\infty$, along the centerline of ribbed floor in five test channels obtained at $Re_d$ = 21,000. The patterns of streamwise distributions depicted in Fig. 4 follow the general trends revealed in Fig. 3, except in the channel of $w/b$ = 2.5 where the streamwise increase of $Nu_d/Nu_\infty$ develops over the plain entry length onto the repeated flow levels of about 2.5. It is worth of noting that the increase of channel $w/b$ ratio at a fixed value of $Re_d$

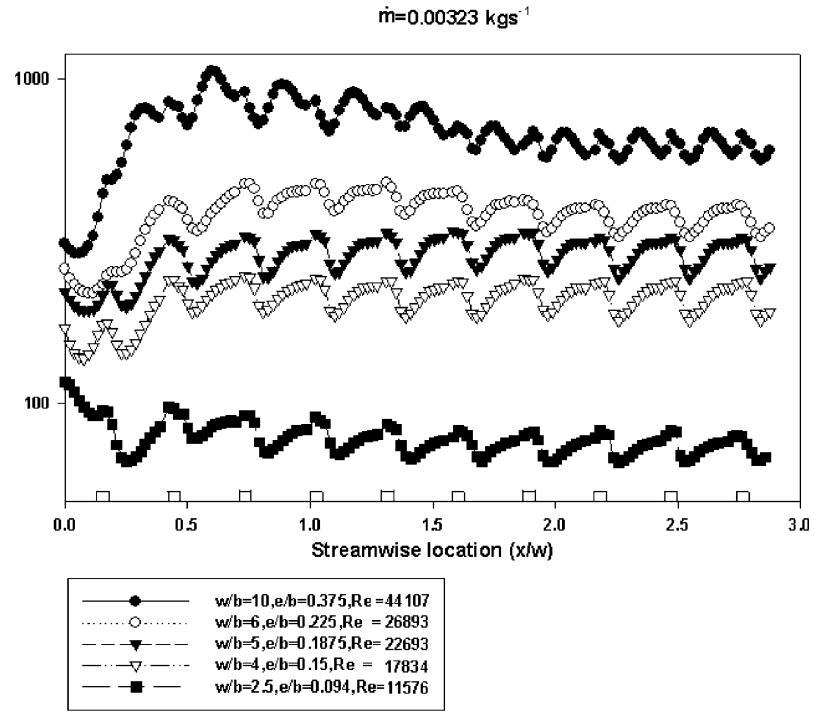


Fig. 3. Streamwise distributions of Nusselt number in five test channels along centerline of ribbed floor at coolant mass flow rate of 0.00323 kg/s.

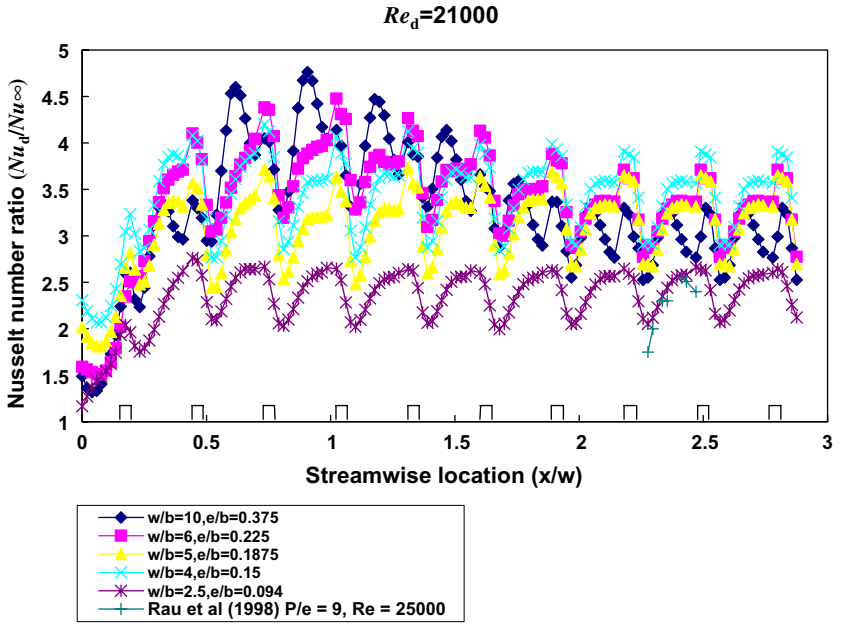


Fig. 4. Streamwise distributions of heat transfer augmentation factor $\frac{Nu_d}{Nu_\infty}$ along centerline of ribbed floor at $Re_d$ of 21,000.

reduces the coolant mass flow rate in order to accommodate the reduced cross-sectioned area. The data of Rau et al. [4] obtained at $Re_d = 30{,}000$ in a squared sectioned ribbed channel is also compared with the present data obtained from the test channel of $w/b = 2.5$. The general agreement between these two sets

Table 2
Correlative coefficients $m$, $m_d$ and $n$ in five test channels

| Tested module | $w/b$ ratio | $e/b$ ratio | $e/d$ ratio | $\overline{Nu} = mRe^n$ | | |
|---|---|---|---|---|---|---|
| | | | | $\overline{Nu}_d = m_d Re_d^n$ | | |
| | | | | $m$ | $m_d$ | $n$ |
| A | 2.5 | 0.094 | 0.066 | 0.1346 | 0.1058 | 0.73 |
| B | 4 | 0.15 | 0.094 | 0.2182 | 0.1688 | 0.721 |
| C | 5 | 0.1875 | 0.1125 | 0.2595 | 0.1864 | 0.709 |
| D | 6 | 0.225 | 0.131 | 0.3294 | 0.237 | 0.688 |
| E | 10 | 0.375 | 0.206 | 2.396 | 1.072 | 0.5256 |

of experimental results is confirmed with discrepancies attributed to the different $Re_d$, $e/d$, $P/e$ and $w/b$ ratios.

When the channel $w/b$ ratio systematically increases from 4 to 10, a corresponding reduction in $Nu_d/Nu_\infty$ level at the spot of immediate flow entrance is observed as shown in Fig. 4. Further downstream moving forward to the first rib, the heat transfer enhancement factors, $Nu_d/Nu_\infty$, in the test channels with $w/b$ ratios of 4, 5, 6 and 10 streamwisely increase. Such streamwise increase in $Nu$ proceeds onto the third rib after where the heat transfers gradually evolve into the repeated nature. At $Re_d$ of 21,000, the highest heat transfer enhancement factors of about 3.5 times of $Nu_\infty$ in the repeated flow are developed in the test channel with $w/b$ ratio of 4 as revealed in Fig. 4. A review of the entire data compared in the manner of Fig. 4 confirms a tendency that the $w/b$ ratio offering the highest $Nu_d/Nu_\infty$ value in the repeated flow region increases when the value of $Re_d$ decreases. The repeated flow region is approximated when the spatially averaged Nusselt number over a rib-pair remains almost unchanged with the period and amplitude of streamwise variation in Nusselt number retain in the similar values. This particular flow region approximately develops after flow traverses five sets of staggered ribs. In order to carry out the further analysis in this respect, the local Nusselt numbers obtained in the repeated flow region at each Reynolds number are spatially averaged into $\overline{Nu}_d$. The subsequent regressive analysis for deriving the correlation of spatially averaged heat transfer over the repeated flow region was performed based on the functional structure of

$$\overline{Nu} = mRe^n \tag{1}$$

$$\overline{Nu}_d = m_d Re_d^n \tag{2}$$

The characteristic lengths selected to define the Nusselt and Reynolds numbers in Eqs. (1) and (2) are the width and the hydraulic diameter of test channel, respectively. Table 2 summarizes the correlative coefficients, $m$, $m_d$ and $n$ obtained in five test channels. The maximum discrepancies between correlated results and experimental data are controlled within the range of ±10%. The exponent $n$ depicted in Table 2 consistently decreases when the $w/b$ ratio increases. As the smooth-walled turbulent flow scenario is recast when $w/b$ ratio approaches zero due to the zero value of $e/b$, a tendency for the $n$ exponent approaching 0.8 at the asymptotic limit of $w/b \to 0$ is observed. Accompanying with the decreased $n$ exponent is the increased coefficients $m$ and $m_d$ when the channel height systematically reduces. The variation manners of the coefficient $m$, $m_d$ and the exponent $n$ with $w/b$ ratio respectively reveal the enhanced rib effect and weakened convective inertia force effect on heat transfer when the channel height thickness reduces. It is demonstrated that the combined effects of channel aspect ratio and rib height to channel width ratio due to variation of channel height for fixed rib-floor geometry have considerable influences on the $m$, $m_d$ and $n$ values. Therefore, the selection of optimal $w/b$ ratio that provides the maximum heat transfer augmentation is $Re_d$ dependent.

## 4. Conclusion

The twofold geometric variations induced by varying the channel height, namely the $w/b$ and $e/b$ ratios, have demonstrated their combined effects on heat transfer. At the fixed coolant mass flow rate, the decrease of channel height consistently improves heat transfers in the present $Re$ range. Heat transfer augmentation is accompanying with a streamwise heat transfer ripple in each rib pair with the peak values developed on the rib top-surface. Over the back edge of each rib, heat transfers fall radically within the bandwidth of about 0.5–1 rib height to a locally minimum value. In the channel of $w/b = 10$, the opposite wall effect triggers the mid-rib heat transfer ripple which has led to twin ripples with equivalent Nusselt number peaks over each rib-pitch in the repeated flow region. In conformity with the experimental results, the proposed heat transfer correlation permits the interactive effects of $w/b$ and $e/b$ ratios on heat transfer over the repeated flow region to be evaluated. The variation manners of the correlative coefficients $m$ and $n$ with $w/b$ and $e/b$ ratios unravel the enhanced rib effect and weakened convective inertia force effect on heat transfer when the channel height

reduces. Therefore the selection of channel *w*/*b* ratio that provides the maximum heat transfer augmentation for the present rib-floor geometry becomes Reynolds number dependent.

## References


[1] J.C. Han, Heat transfer and friction characteristics in rectangular channels with rib turbulators, ASME J. Heat Transfer 110 (1988) 321–328.

[2] T.M. Liou, J.J. Hwang, S.H. Chen, Simulation and measurement of enhanced turbulent heat transfer in a channel with periodic ribs on one principal wall, Int. J. Heat Mass Transfer 36 (1993) 507–517.

[3] M.E. Taslim, T. Li, D.M. Kercher, Experimental heat transfer and friction in channels roughened with angled, V-shaped, and discrete ribs on two opposite walls, ASME J. Turbomachinery 118 (1996) 20–28.

[4] G. Rau, M. Çakan, D. Moeller, T. Arts, The effect of periodic ribs on the local aerodynamic and heat transfer performance of a straight cooling channel, ASME J. Turbomachinery 120 (1998) 368–375.

[5] B. Bonhoff, S. Parneix, B.V. Johnson, J. Schabacker, A. Bölcs, Experimental and numerical study of developed flow and heat transfer in coolant channels with 45 degree ribs, Int. J. Heat Fluid Flow 20 (1999) 311–319.

[6] F.W. Dittus, L.M.K. Boelter, Calif. Pubs., Engng. 2 (1930) 443.

[7] L.M. Su, S.W. Chang, C.I. Yeh, Y.C. Hsu, Heat transfer of impinging air and liquid nitrogen mist jet onto superheated flat surface, Int. J. Heat Mass Transfer 46 (2003) 4845–4862.

[8] Editorial Board of ASME J. Heat Transfer, J. Heat Transfer Policy Report. Uncertain. Exp. Measurem. Results, ASME J. Heat Transfer 115 (1993) 5–6.

[9] D.K. Tafti, Large-eddy simulation of heat transfer in a ribbed channel for internal cooling of turbine blades, in: Proceedings of ASME/IGTI Turbo Expo, GT2003-38122, Atlanta, GA, USA, 2003.

[10] K.R. Farhadi, An experimental investigation of the combined effect of rotation and internal ribbing on heat transfer in turbine rotor blade cooling channels, Ph.D. thesis, University Wales, Swansea, 1993.

[11] P.K. Panigrahi, S. Acharya, Mechanisms of turbulence transport in a turbine blade coolant passage with a rib turbulator, ASME J. Turbomachinery 122 (1999) 152–159.

[12] J. Cui, V.C. Patel, C.-L. Lin, Large eddy simulation of turbulent flow in a channel with rib roughness, Int. J. Heat Fluid Flow 24 (2003) 372–388.